

AUTOMATED POLYP SEGMENTATION IN COLONOSCOPY IMAGES

Swagat Ranjit

*Department of Computer Science and Engineering
Louisiana State University
Baton Rouge, Louisiana, United States*

Bijaya B. Karki

*Department of Computer Science and Engineering
Louisiana State University
Baton Rouge, Louisiana, United States*

Jian Zhang

*Department of Computer Science and Engineering
Louisiana State University
Baton Rouge, Louisiana, United States*

Abstract—It is important to find the polyps in a human system that helps to prevent cancer during medical diagnosis. This research discusses using a dilated convolution module along with a criss cross attention-based network to segment polyps from the endoscopic images of the colon. To gather the context information of all pixels in an image more efficiently, criss-cross attention module has played a vital role. In order to extract maximum information from dataset, data augmentation techniques are employed in the dataset. Rotations, flips, scaling, and contrast along with varying learning rates were implemented to make a better model. Global average pooling was applied over ResNet50 that helped to store the important details of encoder. In our experiment, the proposed architecture’s performance was compared with existing models like U-Net, DeepLabV3, PraNet. This architecture outperformed other models on the subset of dataset which has irregular polyp shapes. The combination of dilated convolution module, RCCA, and global average pooling was found to be effective for irregular shapes. Our architecture demonstrates an enhancement, with an average improvement of 3.75% across all metrics when compared to existing models.

Index Terms—Endoscopic images, Dilated convolution, Criss cross attention, ResNet50

I. INTRODUCTION

One of the most common cancers diagnosed in the western countries and United States is CRC. The factors that might lead to it are smoking, unhealthy diet, high alcohol consumption, physical activity, and excess body weight [2]. It can be prevented early through regular checkups, surveillance and high quality treatment. According to American Cancer Society, 106970 new cases of colon cancer were found in the United States for 2023. They estimated that 1 in 23 for men and 1 in 26 for women have chances of developing colorectal cancer in their lifetime. The death rates are also increasing 1% annually in 50 years or younger population and by 0.6% among 50-54 age group since 2005 [2]. Polyp is the abnormal growth of tissue that develops in mucosal layer of the colon, or intestine. Some polyps are cancerous while others are not. Polyps can potentially develop into colorectal cancer. Polyps in the intestinal tissues are precursors of CRC and can easily turn into malignant lesions [1]. The survival rate depends on how far the cancer from the polyps has spread in the body. It

is decreased from 91% when detected in early stage to 14% in later stage [4]. Therefore, it becomes important to detect the polyp as early as possible.

The primary objective of this research is to evaluate the usefulness of RCCA in image segmentation and design a model with more accurate and efficient segmentation techniques in polyp segmentation tasks. RCCA has been applied in various scenarios with superior results. This research specifically concentrates on assessing its effectiveness in these kind of medical segmentation tasks. The detection and segmentation of polyp require manual work in a regular clinical practice. This approach has not been effective with many examination procedures. Hence, there is a need for systematic and automatic polyp segmentation to assist the medical professionals. To overcome these challenges, deep learning-based segmentation models warrant further investigation.

Still, polyp segmentation task with the help of computer-assisted techniques is a difficult task because of different shape and size of polyps at different stages of development. In the earlier stage, the polyps are often small, lack distinctive features and can be easily missed out. Their size and shape changes as they grow in later stages. Furthermore, the appearance of polyps can differ depending on camera angle. This might not have clear boundaries with neighbor tissues and can be obscured by other regions in the intestine. These factors pose challenges in accurately segmenting polyps. This research is motivated by the limitations of existing methods mainly on irregular polyp shapes. This research presents a new architecture that can be implemented in this type of problem.

Colonoscopy is an effective approach used by the medical professionals that is used to identify the location of polyps, and remove them before leading to cancer. The identification and segmentation of these polyps during colonoscopy require manual work by doctors. Thus, it is crucial to accurately detect and identify polyps as early as possible. Detection at the early stage is a very crucial task that is carried out by experienced professionals through colonoscopy [3]. Figure shows the 5-year survival rate for early stage of colorectal cancer. It indicates that the chances of survival is 90% (very high) if it

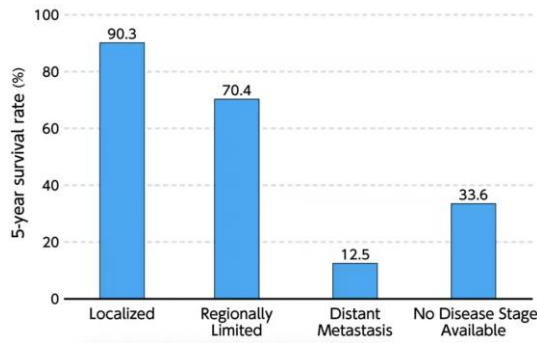


Fig. 1. 5-year survival rate for colorectal cancer by stage

is diagnosed early. But, medical professionals might sometime miss the polyp due to some technical or unseen errors. Therefore, automated polyp segmentation methods are needed to assist clinicians in accurate diagnosis. Machine learning models can help the medical professionals and patients.

II. RELATED WORK

In this chapter, we discuss about the summary of existing methods that was employed over the time. Most of these approaches are categorized based on their shape, texture and deep learning techniques.

A. Polyp Segmentation Based on Texture

The general approach for this type of segmentation task involves various computational methods to analyze the texture characteristics of polyps. Larger polyps in the colon often have more blood in them, which makes them look redder than the nearby tissues. This redness helps to identify these polyps apart from surrounding tissues in the colon. So, this texture characteristic can be helpful to distinguish between these two regions. A. Gonzalez et al. [13] proposes a architecture that extracts texture features from colonoscopy image for polyp segmentation. They used Gray-Level Co-Occurrence Matrix (GLCM) and Local Binary Patterns (LBP) for texture feature extraction and WEKA software for feature selection and classification using random forest. This method achieved most polyp detection rate, and annotated area coverage as compared to other texture based method. Similarly, K. Bora et al. [14] focused on polyp detection using texture, and color features. They used MATLAB and SPSS for their experiments, applying statistical methods for feature selection. The classification involved GLCM, LBP, and color moments. For the best results, they used Non-Subsampled Contourlet Transform (NSCT) filters, particularly 'pyrex' and 'pkva', which showed high accuracy in classifying polyps. The study concluded that these NSCT filters and shape features are independent and effective for polyp classification.

B. Polyp Segmentation Based on Shape

Generally, polyps have clear geometric characteristics like edge, shape can help to identify and delineate it from the surrounding tissue. In [6], they proposed a new method on the

basis of ellipse shape rather than texture. At first, they used watershed algorithm to determine whether elliptical shapes can fit in the polyp region. Then, a method was introduced to distinguish polyp and non polyp region based on curve direction, and edge. [7] employed a hybrid shape-context approach, combining the contextual information to eliminate non-polyp regions and shape information for accurate polyp localization. Initially, a crude edge map was obtained and non polyp regions are distinguished with the help of distinctive feature extraction and edge classification scheme, followed by the localization of polyp candidates using a voting scheme and probabilistic confidence scores in the refined edge maps.

These methods are based on the fact that polyps possess a clearly defined delineated form. But, it is not always the case. In [8], Breier introduces Chan-Vese algorithm which is active contour model that do not depend on gradient information in the image. This was found to be effective in fitting the polyp contours correctly. But, it typically requires a manual setting during initial contour position and hence, this method is not fully automatic.

C. Polyp Segmentation Based on Deep Learning Models

Polyp segmentation is one of the important challenge since the introduction of computer vision. Different convolutional neural networks in the form of U-Net has been introduced and extended over the years. E. Ribeiro et al. [5] utilized Convolutional Neural Networks (CNN) that focuses on exploiting texture patch classification and uses small patches to enhance the database size. It showed higher efficiency compared to common features used for polyp classification. Guo et al. [12] presented a new approach of integrating Feature Enhancement in U-Net which eliminates the problem of image sizes and shapes. They used different standard datasets and improved the performance in terms of 7.7% in Dice Similarity Coefficient and 5.6% in Mean Intersection over union as compared to the existing models. In [9], an end-to-end full convolutional neural network was utilized in the CVC-ClinicDB datasets. The network involved a feature extraction stage, which isolated low-level features, and it was used in prediction map reconstruction stage, which restored the features to the original image size. This approach yielded improved accuracy of 96.98%, F1 score 83.01% and sensitivity values of 77.32%. J. Lewis et al. [11] employed a dual encoder-decoder which is the combination of deep learning models like multiple encoders and decoders along with the transformer. This architecture solved the challenges arising from specular reflections in colonoscopy images. Poorneshwaran et al. [10] proposed a new pix2pix conditional generative adversarial network for solving the polyp segmentation problem. It contains a generator network that employs U-net for segmentation, and a discriminator network for learning and calculating a loss function. They worked on CVC-Clinic dataset and accomplished Dice index 88.48% and Jaccard index 81.27%.



Fig. 2. Kvasir images

III. POLYP DATASET

The polyp dataset used in this thesis research was Kvasir, which consists of intestine polyp images. This dataset is collected with the help of endoscopic equipment at Vestre Viken Health Trust in Norway [15]. It contains manually annotated masks, validated as ground truth by medical experts. These polyp images are taken from colonoscopy videos and contains different types and sizes of polyps. The size of image dataset was in the range from 332x487 to 1920x1072 pixels. As deep learning models require fixed input dimensions, images were resized to 720x576 pixel RGB format. Figure 4.1 shows the Kvasir dataset images. Here, the mask images use two colors: white indicates the presence of polyp and black indicates the background of image as shown in figure 4.2. It consists of 1200 images and mask which is used for this research. This dataset contains high-quality images suitable for medical image analysis.

IV. DATA PREPROCESSING

Normally, the KVASIR dataset has images containing different types, sizes, and noise which have negative impact in the performance of the model. So, we need the image preprocessing before we fed the data to the network. To overcome the issue of overfitting, we employed different contrast, rotations, flips, scaling, and gaussian noise as shown in figure 4.3. In the research, different angles of rotation is used to ensure that the model doesn't become dependent on a specific angle during training process. It undergoes a rotation process around its center and both rotation and shifting are achieved in this process. A high dimensions of images leads to increases the feature map size which results in high memory storage and execution time. So, the images was resized to standard 256 * 256 pixels and helped to make a deeper CNN model.

V. PROPOSED METHOD

A. Encoder with Dilated Convolution Layer Module

Firstly, we perform the transfer learning with pre-trained Res-Net50 with COCO dataset as backbone for the feature extraction in the encoder side. The backbone feature, f_b 'is

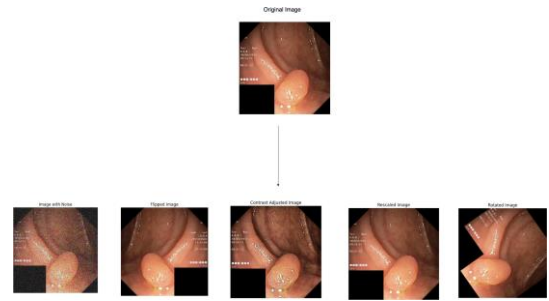
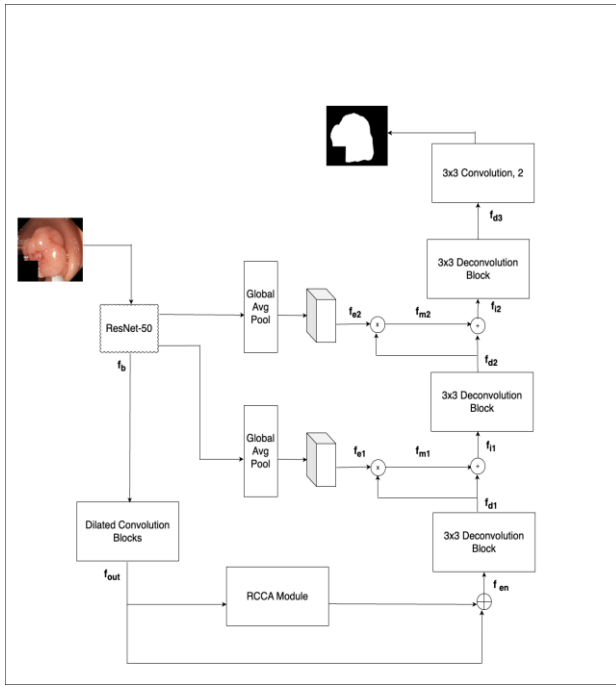


Fig. 3. Data pre-processing

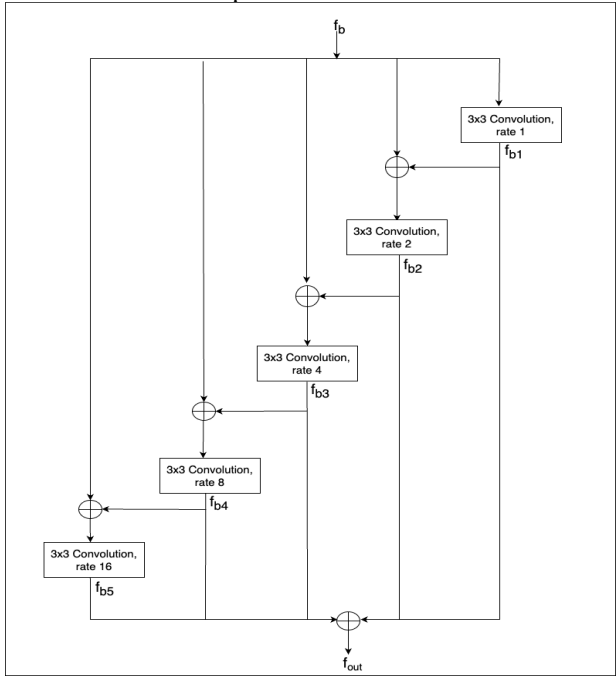
passed to the module which contains multiple dilated convolution layer with different dilated rates. The main advantage of it is the increase in receptive field of the layers without expanding the number of hyperparameters. With the help of different dilation rates, the dilated convolutions can easily aggregate information from a larger area of the input. It is helpful for understanding the larger contexts of image in tasks such as segmentation. Also, it doesn't reduce the size of convolutional kernel. It decreases the dimension of the feature map after the traditional convolution layers has been applied. But, dilated convolution preserve or enhance the spatial resolution of feature maps. At first, 3x3 dilated convolution with dilation rate 1 is applied to produce new dilated feature, f_{b1} '. This new feature f_{b1} ' is concatenated with original backbone feature f_b '. The output of this concatenation serves as input to the next 3x3 convolution with dilation rate 2. It produces new larger dilated feature f_{b2} ' with larger receptive fields. This larger receptive fields plays an important role to catch the features of input image at multiple scales. Similarly, it is concatenated with original feature and it is passed to another convolution layer with different rate. It is repeated for dilation rates 4, 8 and 16 to make f_{b3} ', f_{b4} ', and f_{b5} ' respectively. These rates are important parameter that reveals how convolutional kernel is applied to the input. The dilated convolution functions as standard convolution if the dilation rate is 1. As the rate increases, the gaps is created between the kernel elements which enlarges the kernel's view. Hence, a higher dilation rate expands the receptive field without increase the resources. This helps the model to aggregate the information over larger areas of input kernel. Finally, all new dilated features are concatenated to output the new dilated feature, f_{out} '.

B. Recurrent Criss Cross Attention Module

Criss cross module [16] gathers the contextual information of each pixel in both vertical and horizontal directions. It is designed to capture the long range contextual information in images more efficiently than traditional global attention mechanisms. Input images, X with a number of channel (C), height (P), and width (W) are passed through convolutional layers to create many simplified images, known as feature maps, H. Downsampling operations was utilized to output the feature map H with 1/8th reduction of original image. Further,



Proposed Architecture



Breakdown of Dilated Convolution Block

Fig. 4. Polyp Segmentation Model along with its component

criss-cross attention module on H was introduced to make new feature maps H' . The global contextual information is gathered for each pixel that lies in same row and same column. This new feature map is again passed to the criss-cross attention module once more, resulting in new feature map H'' where every point in H'' collects data from all pixels. However, it doesn't cover for the relationship between a pixel and its neighbouring pixels that doesn't lie in criss cross directions. To

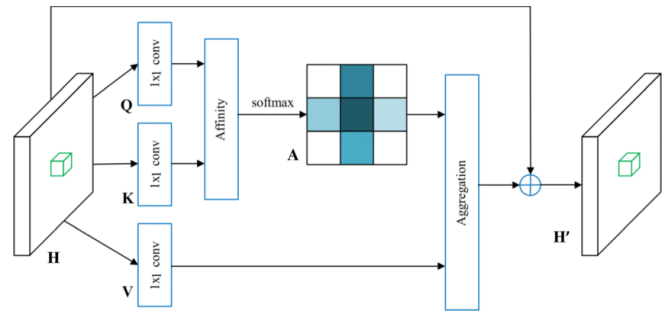


Fig. 5. Criss-Cross Attention Module [16]

solve these issues, a new operation called RCCA is introduced where criss cross attention is applied multiple times. The CCA modules, positioned both before and after in the sequence, utilize same parameters to minimize the additional parameters. This repeated use of the module is termed as Recurrent Criss-Cross Attention (RCCA) module.

In Figure 4.5, criss-cross attention module is shown along with a feature map H . At first, it uses two convolutional layers with small 1×1 filter on feature map $H \in R^{C \times P \times X \times W}$ that creates Q and K feature maps, where $K, Q \in R^{C' \times P \times X \times W}$. Both K and Q have fewer channels than M (C') but they have the same height and width. Then, an attention map A is calculated by applying affinity operation and a softmax function. The affinity operation helps to find how similar the features at different positions are related to each other. Here, the affinity is interpreted as:

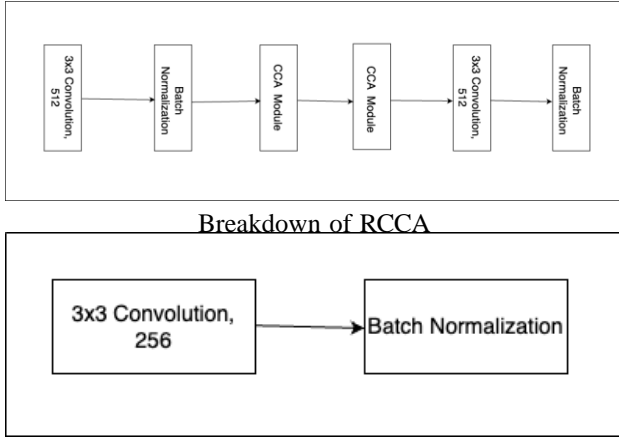
$$d_{i,u} = Q_u W_{i,u}^T$$

where $d_{i,u} \in D$ is the degree of correlation between Q_u and $W_{i,u}$. $i = [1, \dots, |u|]$, $D \in R^{(H+W-1) \times H}$

Similarly, a third convolutional layer with 1×1 filter is applied to M , which outputs a feature map $V \in R^{C \times P \times X \times W}$. V_u and u that are in line with u is extracted at each position u on V . The final step is aggregating the contextual information. This is done by combining the information from attention map A and the vectors in u with the original features at u from M to produce a feature vector $H'u$ in a new feature map H' . This new map H' has richer information because it gathers details from the whole image in a criss-cross manner. As a result, this method effectively collects the contextual details of all pixels in entire image that leads to new feature maps.

In our architecture, the feature ' f_{out} ' is applied with 3×3 convolution and is forwarded to RCCA module. This process is crucial for refining the feature map by extracting the significant patterns. Then, it is passed through batch normalization to stabilize the learning process. This is very effective at capturing important features of images like edges, corners. After applying the convolution layer, batch normalization is employed. It allows this model to learn more consistently without large or small fluctuation of learning rate and efficient learning method. Also, it solves the vanishing gradients problem. After this initial step, the feature map is passed towards the first RCCA module. RCCA module has the capability to capture the contextual information from the entire image, not only

the surrounding pixels. The first CCA module collects the contextual information from those pixel that lie in same row and column. This approach significantly minimizes the number of weights connection and produces sparse attention maps as compared to traditional method. After this step, a recurrent operation is executed on the first attention map. It helps in identifying the precise boundaries of different shapes of image that needs a understanding of entire image. This recursive step allows each pixel to generate the contextual information from the entire image. Then, it is passed through a convolution layer with 3x3 filter. This step compresses the feature extraction to produce final encoder feature, ' f_{en} '. This feature is passed to the decoder module.



Breakdown of Deconvolution Block
Fig. 6. Components of Proposed Architecture

C. Decoder with Global Average Pooling

The encoder reduces the spatial dimensions of input to represent the high level semantic information. It is downsampling process. Then, the decoder restores the spatial dimensions to reconstruct the finer details of image that is required for pixel-wise segmentation. This process is called upsampling. The native approach during upsampling is to concatenate the encoder and decoder. The concatenation is done between encoder and upsampled decoder feature map. It is used to reestablish the original high resolution lost during the downsampling to the upsampling process. This assists the network to reconstruct the finer details of image more accurately with the help of detailed feature maps. The detection of edges and boundaries becomes very difficult to identify because of variations in image scaling and deformation, as well as polyp region sizes. These factors make it difficult to identify polyp and non-polyp regions. However, when the training dataset is limited, a challenge for the network arises. The decoder can start retaining the details of training images instead of learning new generalized features. This might leads to overfitting of training data. To mitigate this problem, global average pooling concept was introduced to remember the importance of encoded features. Global average pooling is applied to these features at first instead of concatenating the encoder features to decoder.

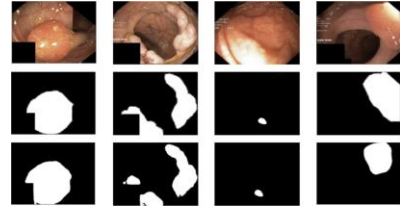


Fig. 7. Results of proposed architecture

Global average pooling reduces feature map to single average value that captures the important detail of feature map and discards the less relevant information. This helps the model to focus on generalized and global features rather than just taking pixel details from training images.

As shown in Fig. 4.4, the decoder has two upsampling processes, each helps to progressively reconstruct the entire image's spatial resolution. In our architecture, encoder feature ' f_{en} ' is passed through 3x3 convolution along with batch normalization. It produces the first decoder feature ' f_{d1} ' in the first upsampling process. The second block of ResNet50 is applied with average global pooling to produce a feature map ' f_{e1} '. It is then operated with pixel-wise multiplication with the first decoder feature ' f_{d1} ' which holds the information of important encoder feature. This new output feature ' f_{m1} ' is applied with pixel wise addition with ' f_{d1} ' to produce first improved feature ' f_{i1} ' which helps to prevent the overfitting of training data. This improved feature ' f_{i1} ' is then upsampled by a scale of 2 to output second decoder feature map ' f_{d2} ' for second upsampling process.

Similarly, the first block of ResNet50 is passed through global average pooling to make a feature map ' f_{e2} '. Then, it is applied with pixel wise multiplication with ' f_{d2} ' to output the second enhanced feature map ' f_{m2} ' which has the main information about the encoder features. ' f_{d2} ' is passed through pixel wise addition with ' f_{m2} ' to have better decoder feature ' f_{i2} '. Finally, it is passed through 3x3 convolution along with batch normalization to get ' f_{i3} ' and another 3x3 convolution with filter size 2. This produces the predicted output.

Experiment Design and Results

VI. IMPLEMENTATION DISCUSSION

For the training of dataset using purposed method, it was further divided into training, and test datasets. Here, 980 training and 220 testing images were employed. Further, the test dataset was divided into two subsets: one comprising irregular shapes (120 images) and the other consisting of regular shapes (100 images). The training was done with 8 batches and maximum 300 epochs. Stochastic gradient decent optimizer with learning rate set to 0.002, weight decay as 0.0005 and momentum as 0.9 is implemented during training.

This thesis work was carried out on LSU HPC clusters that uses python 3 pytorch on Jupyter notebook environment. The computational resources provided contains 2.7GHz 18-core skylake gold 6150 xeon 64-bit processors, two NVIDIA V100 16GB GPU and 384GB DDR4 2666MHz Ram [19].

For evaluation purpose, the recall, precision, accuracy, mean intersection over union, and mean dice are used. It shows the prediction of model as compared to actual ground truth. Higher precision means few false positive and the model is successful in finding only true polyp region. Similarly, high recall implies that the model can detect most polyps, which lowers the false negatives. Accuracy reflects the ratio of correct predictions for polyp and non polyp region among all predictions. IoU measures how well the predicted polyp region overlaps with the actual polyp region. Also, DSC is similar to IoU.

VII. QUANTITATIVE RESULTS

The quantitative results of proposed architecture along with existing models like U-Net [17], HardDNetSeg [18], ConvSegNet [20], MSNet [21], PraNet [22] is shown in Table. The proposed model achieved DSC of 0.8577, mIOU of 0.6914, precision of 0.8893, recall of 0.8472 and accuracy of 0.9652. The results do not show the significant improvement in all metrics except accuracy as compared to other models. It shows the best precision and accuracy among existing models by a small margin. It suggests that the architecture is good at making correct predictions when it classifies a pixel as a part of class. But, mIOU is on low side which indicates the variability performance for different categories. Further, the performance of architecture was evaluated for two subset of the original test dataset. The subset consists of regular and irregular shape polyp images. 110 irregular and 90 regular shaped images were selected for further evaluation and the comparison between them is done. The proposed architecture showed a significant improvement over existing models in irregular polyp shapes.

TABLE I
COMPARISON WITH EXISTING MODELS.

Model	BackBone	DSC	mIOU	Precision	Recall	Accuracy
U-Net	ResNet34	0.8264	0.7472	0.6722	0.6171	0.8936
HardDNetSeg	-	0.826	0.7459	0.8652	0.8485	0.9492
ConvSegNet	ResNet101	0.8618	0.6936	0.8622	0.9124	0.9517
MSNet	Rs2Net50	0.887	0.792	0.847	0.8316	0.9584
PraNet	-	0.898	0.785	0.875	0.901	0.943
Proposed Model	ResNet50	0.8577	0.6914	0.8893	0.8472	0.9652

A. Subset of Irregular Images

The focus of this research is mainly in making better results for irregular shaped polyps. The important component, RCCA helped to enhance the performance of model in this case. It outperformed the existing state-of-models and achieved 0.867 DSC, 0.808 mIOU, 0.926 precision, 0.904 recall and 0.9577 accuracy as seen in last row of Table. There is a significant improvement of average 3.75% among all metrics as compared to existing models as shown in Table. This shows the effectiveness of RCCA in our architecture for polyp segmentation task.

B. Subset of Regular Images

The result of regular polyp images can be observed in below Table. The proposed model did not show the superior results

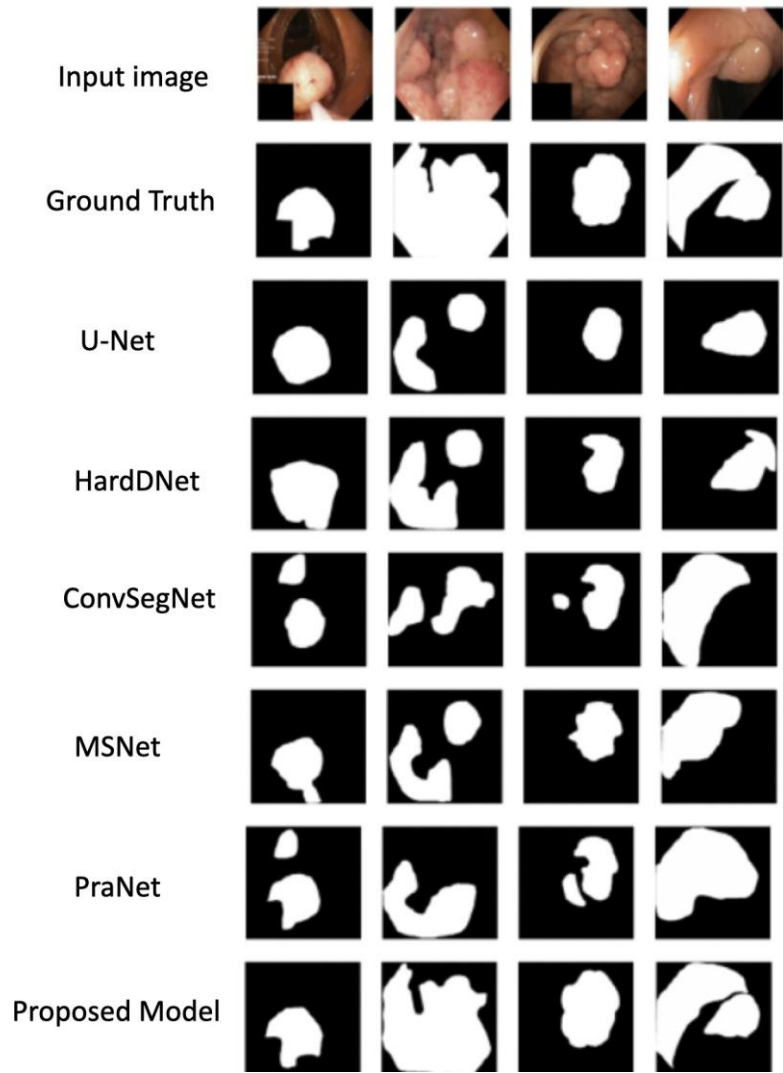


Fig. 8. Results of the proposed architecture in an irregular dataset

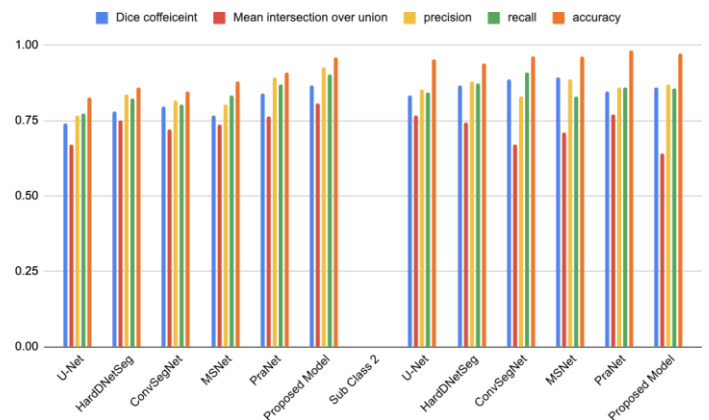


Fig. 9. Graph showing the result of irregular image subset1 and regular image subset2

TABLE II
COMPARISON WITH EXISTING MODELS IN IRREGULAR POLYP SUBSET.

Model	BackBone	DSC	mIOU	Precision	Recall	Accuracy
U-Net	ResNet34	0.739	0.672	0.768	0.773	0.825
HardDNetSeg	-	0.78	0.749	0.837	0.822	0.859
ConvSegNet	ResNet50	0.797	0.721	0.815	0.803	0.847
MSNet	Res2Net50	0.768	0.736	0.802	0.834	0.881
PraNet	-	0.84	0.765	0.893	0.869	0.908
Proposed Model	ResNet50	0.867	0.808	0.926	0.904	0.9577

TABLE III
COMPARISON WITH BEST MODELS IN IRREGULAR POLYPS SUBSET.

	DSC	mIOU	Precision	Recall	Accuracy
Proposed Model	0.867	0.808	0.926	0.904	0.9577
Best Existing Model	0.84	0.765	0.893	0.869	0.908
Difference	0.027	0.043	0.033	0.035	0.0497

like irregular shape as compared to regular shape polyps. ConvSegNet demonstrates the better results with dice coefficient of 88.6%, precision 83%, recall 91.1% and accuracy 96.4%.

TABLE IV
COMPARISON WITH EXISTING MODELS IN REGULAR POLYP SUBSET.

Model	BackBone	DSC	mIOU	Precision	Recall	Accuracy
U-Net	ResNet34	0.833	0.766	0.852	0.884	0.953
HardDNetSeg	-	0.865	0.743	0.881	0.874	0.939
ConvSegNet	ResNet50	0.886	0.67	0.83	0.911	0.964
MSNet	Res2Net50	0.892	0.711	0.885	0.83	0.962
PraNet	-	0.847	0.77	0.859	0.861	0.983
Proposed Model	ResNet50	0.859	0.642	0.868	0.856	0.971

VIII. COMPARATIVE ANALYSIS

The comparative analysis of the performance of the model can be summarized as below:

High DSC and accuracy: As evidenced in the results, both MSNet and the proposed approach exhibit robust overall performance. High DSC means the significant overlap between predicted polyp region and actual ground truth. High accuracy

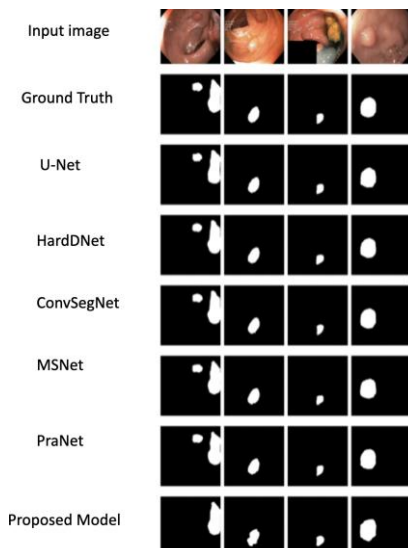


Fig. 10. Graph showing the result of regular image

shows the model ability to correctly classify pixel across categories.

Precision vs. Recall Trade-off: The relationship between recall and precision can be observed from the above comparison table. The higher precision models like proposed model are good that minimizes the false positives. High precision comes at the cost of recall and leads to missing relevant instances. Models with high recall focuses on capturing relevant instances to make accurate prediction which leads to higher false positive.

Balanced Performance: Models like MSNet with Res2Net50 showed a more balanced performance for precision and recall among UNet, PraNet, MSNet, HardDNet, ConvSegNet. It exhibits the ability of model to manage the precision-recall tradeoff which can make it a good choice for image segmentation tasks.

IX. QUALITATIVE RESULTS

Figure 5.1 reveals the qualitative results of the proposed architecture. The first row consists of real colonoscopy images, middle row shows the ground truths, and last row indicates the predicted results. The ground truths of polyp regions are marked by white background.

Similarly, the results of proposed architecture on irregular dataset can be observed in figure 5.2. Proposed model was able to identify the polyp regions more accurately than other models. The bar chart has been shown in Figure 5.3 for both regular and irregular polyp subsets. In this figure, proposed model shows good result in left side of chart which is irregular polyp subsets. Also, PraNet has been more effective in regular shaped polyp images which is in right side of chart.

X. ABLATION STUDY

We explore the effectiveness of various encoder and decoder components by using the proposed architecture. In the ablation study, different combination of components was tested to find its importance. The hyperparameters was same for all different combinations in this experiment. Dice coefficient, mean intersection over union, precision, recall and accuracy were used for measuring the performance. Above table shows the result of ablation study for this research. The combination of 5 layers of dilated convolutions and RCCA is implemented in encoder along with global average pooling in decoder. The integration of all three components gives the best result as observed in fourth row of table. There were four experiments involved which are as follows:

A. Without Global Average Pooling

When both dilated convolution and RCCA is applied, the model shows the result of 0.82 DSC, 0.63344 mIOU, 0.8437 precision, 0.7953 recall and 0.9310 accuracy. This experiment shows good performance but it can be further improved as indicated by DSC and mIOU.

B. Without RCCA

With the combination of Dilated Convolution and Global Average Pooling without RCCA, 0.7654 DSC, 0.5897 mIOU, 0.802 precision, 0.769 recall and 0.9290 accuracy was obtained as observed in second row of table. This combination resulted in unsatisfactory outcome as it decreased all performance metrics as compared to other experiment which shows the important role of RCCA in improving the model performance. This highlights the importance of RCCA in the polyp segmentation for better results.

C. Without Dilated Convolution

Using RCCA in encoder and global average pooling in decoder, it achieved 0.8436 DSC, 0.6631 mIOU, 0.8528 precision, 0.8225 recall and 0.9419 accuracy. It showed the improvement over the above two experiment configurations and suggests that global average pooling and RCCA are important features for polyp segmentation task. It also reveals that dilated convolution is not much effective for capturing the important contextual information for the segmentation task.

D. Inclusion of all Components

The combination of all components gives the best performance across all metrics: 0.8577 DSC, 0.6914 mIOU, 0.8893 precision, 0.8472 recall and 0.9652 accuracy. This shows the importance of improving the model performance that leads to better precision, recall, accuracy, dice coefficient and mean intersection over union.

This ablation study indicates the importance of RCCA that shows the effectiveness in the performance of polyp segmentation models. The integration of these three models showed the effective and best results across all metrics. Dilated convolution captures the receptive field, RCCA uses criss cross attention mechanism and global average pooling in feature aggregation. This integrated approach helps the model's capability to accurately identify the polyp.

TABLE V
ABLATION STUDY.

Dilated Conv.	RCCA	Global Avg. Pooling	DSC	mIOU	Precision	Recall	Accuracy
X	-	X	0.7654	0.5897	0.802	0.769	0.9290
-	X	X	0.8436	0.6631	0.8528	0.8225	0.9419
X	X	X	0.8577	0.6914	0.8893	0.8472	0.9652

XI. CONCLUSION

In this thesis, the proposed deep learning model involving RCCA was able to solve the polyp segmentation challenge. We illustrated the use of dilated convolution layers, RCCA in encoder and global average pooling in decoder to show the effective results in irregular polyp shapes. The original dataset was divided into two subsets based on the shape: Irregular shape with 55% and regular shape with 45%. The main problem of existing model was on irregular shaped dataset. We explored the use of RCCA in these dataset and got better results. The result showed an overall 3.55% improvement across all metrics as compared to other models.

The comparison with existing model in two subsets is also done. Further, we tested the architecture on entire test dataset. However, it didn't demonstrate the best result in it.

In future experiments, we plan to test the performance of our model using different pruning techniques. It helps to evaluate our model by determining how effective model remains when implemented in low cost hardware and limited computational resources. Model pruning allows quantification of efficiency when deployed on constrained hardware with limited computing power. Also, the model can be trained on diverse polyp data and other dataset to better capture different shape, size and location across different stages of progression. Further, the developed polyp segmentation model can be integrated with real-time colonoscopy devices to assist doctors in early identification and diagnosis. This could improve detection rates.

REFERENCES

- [1] J. J. Granados-Romero, A. I. Valderrama-Treviño, et al., *Colorectal cancer: A review*, J. Int. Med. Res., vol. 5, no. 11, pp. 4667-4676, 2017.
- [2] American Cancer Society, *Key Statistics for Colorectal Cancer*, <https://www.cancer.org/cancer/types/colon-rectal-cancer/about/key-statistics.html>.
- [3] American Cancer Society, *Colorectal Cancer Early Detection, Diagnosis, and Staging*, <https://www.cancer.org/cancer/types/colon-rectal-cancer/detection-diagnosis-staging.html>
- [4] Amber J. Tresca, *Stages of Colon and Rectal Cancer*, <https://www.verywellhealth.com/what-are-the-stages-of-colon-and-rectal-cancer-1941590>.
- [5] E. Ribeiro, A. Uhl and M. Hafner *Convolutional Neural Networks 2016 IEEE 29th International Symposium on Computer-Based Medical Systems (CBMS)*, Belfast and Dublin, Ireland, 2016, pp. 253-258, doi: 10.1109/CBMS.2016.39.
- [6] S. Hwang, J. Oh, W. Tavanapong, J. Wong and P. C. de Groen, *Polyp Detection in Colonoscopy Video using Elliptical Shape Feature*, 2007 IEEE International Conference on Image Processing, San Antonio, TX, USA, 2007, pp. II - 465-II - 468, doi: 10.1109/ICIP.2007.4379193.
- [7] N. Tajbakhsh, S. R. Gurudu and J. Liang, *Automated Polyp Detection in Colonoscopy Videos Using Shape and Context Information*, IEEE Transactions on Medical Imaging, vol. 35, no. 2, pp. 630-644, Feb. 2016, doi: 10.1109/TMI.2015.2487997.
- [8] M. Breier, S. Gross, and A. Behrens. *Chan-Vese Segmentation of Polyps in Colonoscopic Image Data*. In Proceedings of the 15th International Student Conference on Electrical Engineering, 2011.
- [9] Q. Li et al. *Colorectal polyp segmentation using a fully convolutional neural network 2017 10th International Congress on Image and Signal Processing, BioMedical Engineering and Informatics (CISP-BMEI)*, Shanghai, China, 2017, pp. 1-5, doi: 10.1109/CISP-BMEI.2017.8301980.
- [10] J. M. Poorneshwaran, S. Santhosh Kumar, K. Ram, J. Joseph and M. Sivaprakasam *Polyp Segmentation using Generative Adversarial Network 2019 41st Annual International Conference of the IEEE Engineering in Medicine and Biology Society (EMBC)*, Berlin, Germany, 2019, pp. 7201-7204, doi: 10.1109/EMBC.2019.8857958.
- [11] Lewis, J., Cha, YJ., Kim, J. *Dual encoder-decoder-based deep polyp segmentation network for colonoscopy images*. Sci Rep 13, 1183 (2023). <https://doi.org/10.1038/s41598-023-28530-2>
- [12] Q. Guo, X. Fang, L. Wang and E. Zhang *Polyp Segmentation of Colonoscopy Images by Exploring the Uncertain Areas* IEEE Access, vol. 10, pp. 52971-52981, 2022, doi: 10.1109/AC-CESS.2022.3175858.
- [13] A. Sánchez-González, B. Garcia-Zapirain, D. Sierra-Sosa and A. Elmaghraby *Colon Polyp Segmentation Using Texture Analysis*, 2018 IEEE International Symposium on Signal Processing and Information Technology (ISSPIT), Louisville, KY, USA, 2018, pp. 579-588, doi: 10.1109/ISSPIT.2018.8642748.
- [14] Bora, K., Bhuyan, M.K., Kasugai, K. et al. *Computational learning of features for automated colonic polyp classification* Sci Rep 11, 4347 (2021). <https://doi.org/10.1038/s41598-021-83788-8>

- [15] K. Pogorelov, K. R. Randel, C. Griwodz, S. L. Eskeland, T. de Lange, et al. *KVASIR: A Multi-Class Image Dataset for Computer Aided Gastrointestinal Disease Detection* in Proc. 8th ACM on Multimedia Systems Conf. (MMSys'17), Taipei, Taiwan, 2017, pp. 164-169, doi: 10.1145/3083187.3083212.
- [16] Z. Huang, X. Wang, L. Huang, C. Huang, Y. Wei and W. Liu *CCNet: Criss-Cross Attention for Semantic Segmentation*, 2019 IEEE/CVF International Conference on Computer Vision (ICCV), Seoul, Korea (South), 2019, pp. 603-612, doi: 10.1109/ICCV.2019.00069.
- [17] O. Ronneberger, P. Fischer, and T. Brox *U-Net: Convolutional Networks for Biomedical Image Segmentation*, Proceedings of the International Conference on Medical image computing and computerassisted intervention (MICCAI), 2015, pp. 234–241.
- [18] C.-H. Huang, H.-Y. Wu, and Y.-L. Lin *HarDNet-MSEG A Simple Encoder-Decoder Polyp Segmentation Neural Network*, arXiv preprint arXiv:2101.07172, 2021
- [19] "Guides - SuperMIC - HPC @ LSU," Louisiana State University High Performance Computing, <http://www.hpc.lsu.edu/wwwhpc-dev/docs/guides.php?system=SuperMIC>. Accessed: March 23, 2024
- [20] D. Jha, S. Ali, N. K. Tomar, H. D. Johansen, D. Johansen, J. Rittscher, M. A. Riegler, and P. Halvorsen *Real-Time Polyp Detection, Localization and Segmentation in Colonoscopy using Deep Learning*, IEEE Access, vol. 9, pp. 40 496–40 510, 2021.
- [21] X. Zhao, L. Zhang, and H. Lu, *Automatic polyp segmentation via multi-scale subtraction network*, in MICCAI, Springer, 2021, pp. 120-130.
- [22] Fan, DP. et al., *PraNet: Parallel Reverse Attention Network for Polyp Segmentation*, Medical Image Computing and Computer Assisted Intervention – MICCAI 2020. MICCAI 2020. Lecture Notes in Computer Science(), vol 12266. Springer, Cham. https://doi.org/10.1007/978-3-030-59725-2_6